33rd Annual International Conference of the IEEE EMBS
Boston, Massachusetts USA, August 30 - September 3, 2011

Blind Forensics in Medical Imaging Based on Tchebichef Image Moments

H. Huang, G. Coatrieux, Member, *IEEE*, H.Z. Shu, *Senior Member, IEEE*, L.M. Luo, *Senior Member, IEEE*, Ch. Roux, *Fellow, IEEE*

Abstract—**In this paper, we present a blind forensic approach for the detection of global image modifications like filtering, lossy compression, scaling and so on. It is based on a new set of image features we proposed, called Histogram statistics of Reorganized Block-based Tchebichef moments (HRBT) features, and which are used as input of a set of classifiers we learned to discriminate tampered images from original ones. In this article, we compare the performances of our features with others proposed schemes from the literature in application to different medical image modalities (MRI, X-Ray …). Experimental results show that our HRBT features perform well and in some cases better than other features.**

I. Introduction

THE sophisticated and low cost tools of the digital age facilitates creation and handling of digital images. In healthcare, image manipulations encompass global image processing like contrast enhancement, brightness adjustment, lossy compression (e.g. JPEG)… or any combinations of them. They are used by the physician during his or her interpretation of the image and also in order to facilitate image sharing like in telemedicine applications. Because these processes may induce loss of important information that supports the diagnosis, one can no longer take the authenticity of images for granted. It is thus important being capable to detect such image modifications especially to inform the practitioner the image he or she observes has been processed, and also when the image comes to medico-legal evidence.

Image forensics techniques and methodologies for validating the authenticity of an image have recently attracted attention. They can, in principle, reconstitute the set of processing operations the image undergone. They allow us to make statements about the image veracity and give clues about the nature of the performed manipulations. Forensic methods can be distinguished in two classes according to the access to a priori knowledge on the original image. For example, some solutions store or watermark within the image some digests or signatures which by comparison with the recomputed ones states about the image integrity [1]. Even though watermarking is an effective tool for verifying image integrity and origins [2], its application requires that a watermark is embedded during image creation, limiting its use to applications where the digital object generation mechanisms have built-in watermarking capabilities. Majority of images captured today are not watermarked. Therefore, there is a strong need to resort to blind image forensic techniques. These techniques work without a priori information and aim at identifying characteristics or evidences left by most image modifications.

A large group of "blind forensic" methods are based on classifier mechanisms. Classifiers are built on some image features to recognize or identify image modification footprints. Avcibas *et al.* [3] developed a detection scheme that discriminates "doctored" images from original ones (i.e. not tampered) based on the training of a classifier with Image Quality Metrics (IQM). Farid *et al.* [4] developed a detection scheme trained to recognize statistical footprints of image modifications within the High Order Wavelet statistics (HOWs). Similarly, Bayram *et al.* [5] proposed to make use of Binary Similarity Measures (BSM), derived from the correlation between the image bit planes as well as binary texture characteristics within one bit plane. It is important to notice that these methods use image features originally proposed for steganalysis whose purpose is to detect stego-images (i.e. image with secret message embedded). In fact, steganography acts similarly to image modification. It affects more or less the image content while not carrying out perceptible distortions into the image [5]. Recently, for the steganalysis purpose, Liu *et al*. [6] proposed a set of image features designed with Histogram statistical properties of the Reorganized Block-based Discrete cosine transform coefficients (HRBD), that outperforms HOWs features. Notice that HRBD has not been yet experimented for image authenticity purpose. This participates also to the originality of this work. It is expected that the features which perform well for steganalysis will also work better than other image features for detecting image modification.

The objective we pursue in this work is to detect if an image undergone or not some "global" image modification like lossy JPEG compression, filtering and so on. For that purpose, we introduce a new set of image features based on Tchebichef moments, features extracted from the image following the same strategy as Liu *et al*. [6]. DCT coefficients and Tchebichef moments have similar properties. However, Tchebichef moments have shown better performances than DCT coefficients in some image processing applications [7]. Thus similarly to HRBD, we will talk about HRBT. We use both set of features to learn classifiers capable to discriminate original images from modified ones. In this works, we

H. Huang, G. Coatrieux and Ch. Roux are with IT. Telecom Bretagne; Inserm U650, France, e-mail: {Hui.Huang, Gouenou.Coatrieux, Chiristian.Roux}@telecom-bretagne.eu.

H. Z. Shu, L. M. Luo are with LIST Southeast University, China, e-mail: {shu.list, luo.list}@seu.edu.cn.

evaluate and compare our approach (HRBT) with IQM [3], HOWs [4], BSM [5] and HRBD [6] solutions in application to different medical image modalities: X-Ray, Ultrasound and Magnetic Resonance Imaging.

The rest of this paper is organized as follows. Section 2 remembers the basic principles of blind forensic mechanisms for digital image. Section 3 details the proposed method while section 4 provides some experimental results. Conclusions are given in section 5.

II. Blind Forensics for Image

A. Basic Principles

Whatever its extent, any image processing will leave evidences of its application like some image features statistical irregularities. One approach proposed to catch up these evidences is based on the learning of classifiers whose input are image features impacted by image modification. Once the classifier learned, one just has to extract these features from the image under investigation, and to provide them to the classifier for analysis and decision. Efficiency of such an approach largely depends on: i) the design of proper image features and, ii) the way the classifier is built.

In the following, in order to only evaluate features' efficiency, we used Support Vector Machines [8] for the design of classifiers. SVM is one of the most popular supervised classification methods due to its superior classification performances in many applications.

B. Image Features for Blind Forensics

Features we are looking at should reflect changes in an image while being content independent. Image modifications we wish to detect don't impact image main structures but rather image details. In this section, we present some common features proposed for modification detection.

1) Image Quality Metrics (IQM)

In [3], Avcıbas *et al.* proposed to compute IQMs on the signal of difference between the image under investigation and a reference image. In fact, they show that it is possible to find distance measurements between images that can isolate signal changes regardless of image content. In particular, they demonstrate that the first two statistical moments of the angular correlation and of Czenakowski similarity measures satisfy such independency constraint. The reader may refer to [3] for more details. Nevertheless, because in the following experiments, we only work with gray scale images of $N \times N$ pixels, the angular correlation Avcibas *et al.* measure between color components is constant and cannot be exploited. Thus IQMs we consider in our experiments are the two first order statistics of Czekanowski similarity measure. Considering an image under investigation $f(i,j)$ and a reference image $g(i,j)$, these features can be defined as:

$$d_1 = \left[\frac{1}{N^2}\sum_{i,j=0}^{N-1}\left(\chi_{ij} - \mu_\chi\right)^2\right]^{1/2} \tag{1}$$

where: $\chi_{ij} = \frac{2f(i,j)\cdot g(i,j)}{f(i,j)+g(i,j)}$; $\mu_\chi = \frac{1}{N^2}\sum_{i,j=0}^{N-1}\left|\chi_{ij}\right|$, and

$$d_2 = \left[\frac{1}{N^2}\sum_{i,j=0}^{N-1}(v_{ij} - \mu_v)^2\right]^{1/2} \tag{2}$$

where $v_{ij} = \frac{f(i,j)}{2(g(i,j)+f(i,j)\times g(i,j))}$; $\mu_v = \frac{1}{N^2}\sum_{i,j=0}^{N-1}\left|v_{ij}\right|$

2) High Order of Wavelet Statistic (HOWs)

Farid *et al.* benefit from the wavelet decomposition to isolate image details [4]. They propose to discriminate modifications through their impact on the statistical distribution of wavelet coefficients and of their prediction error within wavelet sub-bands. If $V_p(i,j)$, $H_p(i,j)$ and $D_p(i,j)$ denote the coefficients in the vertical, horizontal and diagonal sub-bands at position (i,j) of resolution p respectively, then the estimator of the coefficient $V_p(i,j)$ is:

$$\begin{aligned}\left|\hat{V}_p(i,j)\right| &= \omega_1\left|V_p(i-1,j)\right| + \omega_2\left|V_p(i+1,j)\right| + \omega_3\left|V_p(i,j-1)\right| \\ &+ \omega_4\left|V_p(i,j+1)\right| + \omega_5\left|V_{p+1}(i/2,j/2)\right| \\ &+ \omega_6\left|D_p(i,j)\right| + \omega_7\left|D_{p+1}(i/2,j/2)\right|\end{aligned} \tag{3}$$

where weight $\omega_i \in \Re$. Statistical measurements – the mean, the variance, the skewness and the kurtosis – on wavelet coefficients and on their error of prediction in each sub-band constitute the HOWs features. Readers can refer to [4] for more details on the computation of weight (ω_i) and features.

3) Binary Similarity Measures (BSM)

These measures have been proposed considering the fact that image modifications may induce correlation variations between and within bit planes. These changes can be point out by statistical features extracted from image bit planes. The measures are based on the comparison of binary texture statistics between bit plane pairs of the images (e.g. 5-6, 6-7, 7-8 bit planes). Due to the limited size of the paper, we cannot present details of BSM features. The reader may refer to [5] for their description

4) Histogram Statistics of Reorganized Block-based DCT Coefficients (HRBD)

These features have been proposed for the steganalysis purpose but not yet experimented for image integrity verification. Harmsen *et al.* [9] and Shi *et al.* [10] show up that the center of mass and the higher order statistic moments of the Discrete Fourier Transform of the DCT coefficients Histogram (DFTH) vary after information embedding. Different set of such features have been proposed, Shi *et al.* [10] make use of the HDFT defined as:

$$M_n = \left(\sum_{k=0}^{N/2} k^n |H(k)|\right) / \left(\sum_{k=0}^{N/2} |H(k)|\right), \quad n = 1,2,3 \tag{4}$$

where $H(k)$, $|H(k)|$ denote the DFTH at the frequency k and its magnitude respectively. Wang *et al.* [11] improves steganalysis performances working on filtered version of the DFTH extracting three distinct features $f_i, i = 1 \ldots 3$

$$f_1 = \sum_{k=0}^{K/2} |H(k)| \cdot \sin(\pi k/K) \tag{5}$$

$$f_2 = \sum_{k=0}^{K/2} |H(k)| \cdot \sin^2(\pi k/K) \tag{6}$$

$$f_3 = \sum_{k=0}^{K/4} |H(k)| \cdot \sin(\pi k/K) \tag{7}$$

Liu *et al.* suggest extracting these both set of features from the image and from its difference with its predicted version. They compute them on the DFTH of DCT coefficients regrouped or reorganized in independent "sub-bands" of an L-scale wavelet-like tree [6]. Because we follow the same reorganization procedure with Tchebichef moments, we detail it in section III. Anyway, the prediction algorithm used in the sequel is expressed as [12]:

$$e = x - \hat{x} = \begin{cases} max(a,b) & c \leq min\,(a,b) \\ min(a,b) & c \geq max\,(a,b) \\ a+b-c & otherwise \end{cases} \quad (8)$$

where e is the prediction error of the pixel x; $\hat{x}$ is the predicted value of x; a, b and c are the pixels surrounding x (see Fig. 1).

x	a
b	c

Fig. 1. The neighborhood of the prediction

III. Proposed Image Moment based Feature

A. Image moment

Introduced by Hu [13], one general image moment Ψ_{nm} is defined with a basis function $\varphi_{nm}(x,y)$, and an image intensity function $f(x,y)$such as:

$$\Psi_{\mathrm{nm}} = \iint \varphi_{\mathrm{nm}}(x,y) f(x,y)\,dx dy\,, n, m = 0, 1, 2, \ldots \quad (9)$$

Different types of moments can be defined depending on φ_{nm}. Among these moments, Tchebichef moments are the simplest discrete orthogonal moments, widely used in digital image processing such as image reconstruction and pattern recognition.

The $(n+m)^{th}$ order Discrete Tchebichef moment T_{nm} is defined as [7].:

$$T_{nm} = 1/\rho(n,N)\rho(m,N) \cdot \sum_{x=0}^{N-1} \sum_{y=0}^{N-1} t_n(x) t_m(y) f(x,y) \quad (10)$$

where $t_n(x)$ and $t_m(y)$ are the Tchebichef orthogonal polynomials and $\rho(n,N)$ weighted values:

$$t_n(x) = n! \sum_{k=0}^{n} (-1)^{n-k} \binom{N-1-k}{n-k} \binom{n+k}{n} \binom{x}{k} \quad (11)$$

$$\rho(n,N) = (2n)! \binom{N+n}{2n+1} \quad (12)$$

It is possible to derive the DCT basis from the discrete Tchebichef moments [14]. Some experimental results given in [7] illustrate a close similarity between performances of DCT and Tchebichef moments for lossy image compression and image reconstruction. Sometimes Tchebichef moments provide better reconstruction performances. This motivates us to consider Tchebichef moments as image features.

B. Proposed features

Considering the intrinsic properties of Tchebichef moments, we adapted the strategy of Liu *et al*. [6] to extract our set of features.

In a first time, the image of size *N*×*N* is divided into small blocks of *n*×*n* pixels - in the sequel *n*=8 - and for each, Tchebichef moments up to $((n-1)+(n-1))^{th}$ order ($T_{pq}, p = 0, \ldots, n-1; q = 0, \ldots, n-1$) are computed leading to *n*×*n* moments values. In Fig. 2, T_{pq} is at the coordinate position $(p+1, q+1)$.

In a second time, each block of *n*×*n* moments is partitioned into an *L*-scale wavelet-like tree (see Fig. 2a), within a $3L + 1$ subbands decomposition, where $n = 2^L$.

At last, moments belonging to the same sub-bands in each block are clustered forming an *L*-scale coefficients tree for the whole image. As shown in Fig. 2b, the “sub-band” G0 regroups T_{00} moments of all the blocks in the image, moments that are placed at the same relative positions in the image.

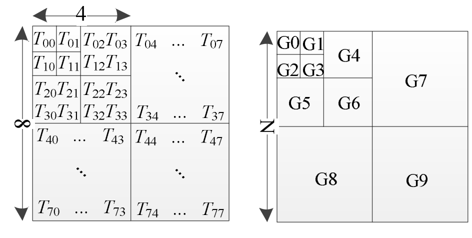

(a) (b)

Fig. 2. Reorganization of block-based Tchebichef moment for an image of *N*×*N* pixels. (a) 8×8 pixel block partitioned as the 3-scale wavelet-like tree. (b) sub-band construction based ob 8×8 block to form a L-scale wavelet like tree of global dimension *N*×*N*.

Our HRBT features are then computed within $\{G_0, G_1, \ldots, G_{3L}\}$ sub-bands of the test image and its predict-error image with equations (4) – (7).

IV. Experimental Results

A. Image test sets

We have used four test sets of images issued from different medical image modalities (see Fig. 3):

- Magnetic resonance images (MRI) of the head: 145 images of 256 × 256 pixels and 12-bit depth,
- Two kinds of X-Ray images: 162 mammograms of 4740×3540 pixels encoded on 12 bits and 135 CT images of 512×512 pixels of 12-bit depth.
- Ultrasound images (Echo): 52 images of 576 × 690 pixels and of 8-bit depth.

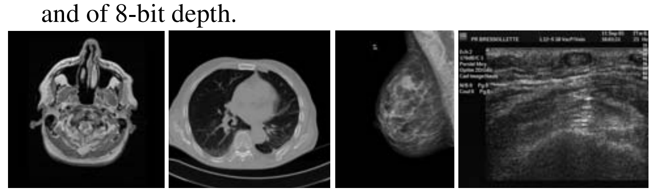

(a) (b) (c) (d)

Fig. 3. Image samples of our test sets: (a) MRI (b) CT image (c) X-Ray image (d) Echography

The modifications we have considered in the experiments are: contrast and brightness adjustment, Gaussian filtering, rotation, compression and histogram equalization. Table I gives the parameters used for each of these modifications. The different image test sets were divided into two groups for classifier learning: a training and a testing group.

B. Performances Evaluation

In this work our goal is only to distinguish original images from modified ones. To achieve this goal, we have learned different SVM based detectors (e.g. original (org.) vs. JPEG, org. vs. filtering …) using our image features. We also built SVM classifiers with the features proposed in [3]-[6]. With this strategy, an image is declared unauthentic, if at least one of our classifiers notifies it.

TABLE II DETECTION RATE ACHIEVED BY DIFFERENT SVM CLASSIFIERS WITH DIFFERENT SETS OF IMAGE FEATURES (IQM, HOWS, BSM, HRBD, HRBT)

Correct Rate (%)		org. vs. all mod.	org. vs. scaling. *	org. vs. rotation	org. vs. filtering	org. vs. adj. cont.	org. vs. brighten	org. vs. JPEG	org. vs. JPEG 2000	org. vs. histo. equ.
MRI	*IQM*	79.46		99.70	54.31	51.11	51.18	49.95	49.93	99.36
	HOWs	81.02	76.67	99.40	97.07	44.79	35.76	56.93	78.06	99.06
	BSM	81.26	99.89	99.60	86.09	73.33	89.23	59.66	96.81	100
	HRBD	82.53	96.26	99.25	96.09	63.12	67.01	99.60	92.85	99.25
	HRBT	83.14	96.38	99.31	97.93	61.11	66.32	95.69	95.35	99.20
Mammography	*IQM*	80.54		100	50.22	52.22	52.04	47.96	47.41	100
	HOWs	79.97	94.38	100	99.91	42.53	33.58	39.14	74.88	93.77
	BSM	81.66	99.81	100	93.81	52.72	53.77	53.89	74.26	99.32
	HRBD	85.74	99.14	100	99.54	63.78	100	100	98.15	99.75
	HRBT	87.11	99.32	100	99.48	62.78	97.90	97.90	98.15	99.75
CT	*IQM*	80.51		100	69.44	54.18	85.90	46.27	44.78	100
	HOWs	81.41	95.97	100	100	54.18	42.69	74.78	97.76	99.18
	BSM	81.09	100	99.70	98.58	82.46	98.13	40.52	89.55	100
	HRBD	88.69	99.70	100	100	92.24	99.40	100	98.51	100
	HRBT	88.50	99.85	100	100	91.34	98.66	99.70	99.25	100
Echography	*IQM*	80.56		100	48.55	59.62	47.88	46.15	48.62	100
	HOWs	85.94	97.12	100	99.84	55.77	58.65	92.69	100	99.81
	BSM	90.29	100	100	97.42	77.69	95.96	90.00	98.85	100
	HRBD	89.06	99.81	100	100	75.19	95.77	100	99.23	100
	HRBT	89.97	100	100	100	73.65	94.04	100	99.04	100

* (not available - IQM characteristics calculation requires access to a reference image of the same dimensions as the original

TABLE I Image manipulation and their parameters

Modification	Values of parameters				
Scaling up(γ_s %)	1	5	10	25	50
Rotation angle(θ)	1	5	15	30	45
Deviation of Gaussian filter (σ)	0.3	0.5	1.0	2.0	3.0
Contrast enhancement rate (γ_c %)	1	5	8	10	
Brighten rate (γ_b %)	2	5	8	10	
Quality factor(Q)	95	85	80	75	60
Compression rate JP2K (γ_j)	2:1	5:1	10:1	20:1	50:1
Histogram equalization					

We consider the detection rate as performance indicator, which is the number of modified and original images correctly detected versus the number of tested images. The results obtained for different detectors are given in Table II.

From the results in Table II, we find out that HRBD and HRBT features can be used for image modification detection and that they have similar performances. HRBT perform slightly better than HRBD except for JPEG, contrast and brighten adjustment. This can be explained by the fact that JPEG quantizes DCT coefficients and that HRBT evolves with such a "gradient variation". Notice that Tchebichef moments have shown better reconstruction abilities for sharp boundary images. It can also be seen that HRBD and HRBT have better behavior than HOWs or BSM in general. Results with IQM features are the lowest in most cases, but they work with only two features while HOWs, HRBD and HRBT handle to 72, 156 and 156 features per image respectively.

V. CONCLUSION

In this paper, we have proposed to use Tchebichef moments to built image features (HRBT) following the strategy of Liu *et al.* (HRBD) for the purpose of verifying medical image integrity. Originally proposed for the steganalysis of natural images, we show up that this approach can also be used for blind detection of global image modification. It outperforms other solutions based on HOWs, IQM and BSM features. Obtained results on different medical image modalities show that our features based on Tchebichef moments perform well on modifications that either affect slightly or strongly the image content. However, they are only slightly better than HRBD features in a few cases, not in all cases as expected. Even so, our proposed method widens the application of Tchebichef moments.

REFERENCES

[1] G. Coatrieux, H. Maitre, and B. Sankur, “Strict integrity control of biomedical images,” in Proc. SPIE on SWMC III, 2001, pp. 229-240.

[2] X. Guo et T.-ge Zhuang, "Lossless Watermarking for Verifying the Integrity of Medical Images with Tamper Localization", Journal of Digital Imaging, vol. 22, no. 6, pp. 620-628, Dec. 2009.

[3] I. Avcibas, S. Bayram, N. Memon, M. Ramkumar, B. Sankur, “A classifier design for detecting image manipulations,” in Proc. Int. Conf. on Image Processing, 2004, vol. 4, pp. 2645-2648.

[4] H. Farid, S. Lyu, “Higher-order Wavelet Statistics and their Application to Digital Forensics,” in Proc. Int. Conf. on Computer Vision and Pattern Recognition Workshop, 2003, vol. 8, pp. 94.

[5] S. Bayram, I. Avcibas, B. Sankur, et N. Memon, "Image manipulation detection", Journal of Electronic Imaging, vol. 15, no. 4, pp. 041102-17, oct. 2006.

[6] S. Liu, L. Ma, H. Yao, and D. Zhao, “Universal Steganalysis Based on Statistical Models Using Reorganization of Block-based DCT Coefficients,” in 2009 Fifth International Conference on Information Assurance and Security, 2009, pp. 778–781.

[7] R. Mukundan, “Transform Coding Using Discrete Tchebichef Polynomials”, Proc. of IASTED Int. Conf. on VIIP 2006, pp 270-275.

[8] L. Wang, Support vector machines: theory and applications. Springer, 2005.

[9] J. J. Harmsen and W. Pearlman, “Steganalysis of additive noise modelable information hiding,” in Proc. SPIE Electronic Imaging, 2003, vol. 5022.

[10] Y. Q. Shi, Guorong Xuan, Chengyun Yang et al. "Effective steganalysis based on statistical moments of wavelet characteristic function", in Int. Conf., ITCC 2005, vol. 1, pp. 768-773 .

[11] Y. Wang and P. Moulin, “Statistical modeling and steganalysis of DFT-based image steganography,” in Proc. SPIE, 2006, vol. 6072, pp. 14–24.

[12] M. J. Weinberger, G. Seroussi, and G. Sapiro, “LOCO-I: A low complexity, context-based, lossless image compression algorithm,” in Proc. 1996 Data Compression Conference, 1996, pp. 140–149.

[13] Ming-Kuei Hu, “Visual pattern recognition by moment invariants,” Information Theory, IRE Trans. on, vol. 8, no. 2, pp. 179-187, 1962.

[14] N. Ahmed, T. Natarajan, and K. R. Rao, “Discrete Cosine Transform,” IEEE Trans. Computers, vol. 23, no. 1, pp. 90-93, 1974.